BJRS

BRAZILIAN JOURNAL
OF
RADIATION SCIENCES
09-02C (2021) 01-21

Polymerization Mechanisms of the Gel Dosimeter Type *nPAG* by High Energy X Radiation and Response Curve Determination Employing TRS 398

Hamann[a] J. H., Peixoto[a] J. G.

[a] *Institute of Radioprotection and Dosimetry - IRD / CNEN, 22783-127, Av. Salvador Allende s/n - Barra da Tijuca - Rio de Janeiro - RJ*

e-mail: jhhamann@gmail.com

ABSTRACT

Dosimetry by polymer gel associated with magnetic resonance imaging (MRI) is a promising technique for three-dimensional dose determination in radiotherapy. Understanding effects of the interaction of radiation with the materials that make up the dosimetric solution and the mechanisms of the polymerization process are fundamental. Thus, studies associated with polymer gel dosimetry have been widely developed. The awakening to this type of work is due to the fact that dosimetry by polymer gel is a tool that allows, for example, the three-dimensional analysis of the dose distribution in a given volume. In this article, a literary review was carried out for a better understanding of the mechanisms responsible for the polymerization process of the dosimeter gel. Then, following the protocol presented in TRS 398, samples of *nPAG* dosimeter gel were irradiated in medical linear accelerator with 6MeV X-ray beam energy. Response curve of these samples was obtained through statistical analysis of magnetic resonance images.

Keywords: Response Curve, TRS 398, Polymers, Dosimeter Gel, Radiolysis.

ISSN: 2319-0612
Accepted: 2021-07-26

1. INTRODUTION

Many of techniques recently developed in the field of radiotherapy, such as three-dimensional treatment planning (3D), intensity modulated radiation therapy (IMRT), radiotherapy (conformal and conventional), volumetric modulated arc therapy (VMAT) and image-guided radiotherapy (IGRT), in addition stereotactic radiosurgery have led to an increase in the complexity of radiation oncological treatment. All these techniques are used to reduce the toxicity generated in treatment, by optimizing the dose in the target volume, thus minimizing the irradiation of radiosensitive or healthy structures adjacent to the tumor region. By reducing the irradiation area closest to the target volume, the accuracy of the treatment system as well as the dose absorbed by the tumor volume is increased. In this way, reliable programs are necessary to systematically ensure great quality and reliability on the radiation beam, planning processes, treatment and dose deposition at the target volume [1,2,3].

Radiotherapy dosimetry protocols for evaluation of dose distribution use film dosimetry, thermoluminescent dosimeters (TLDs), optically stimulated luminescence (OSL) ionization chambers, or solid-state detectors. All are two-dimensional methods for dose measurements. These dosimeters do not measure dose distribution in three-dimensional space, restricted only to two-dimensional readings and only at certain points of analysis. Some dosimeters depend on the energy and angular positioning of the radiation beam for correct reading [4].

Therefore, use of such detectors is also associated with additional problems: *(i)* some have relatively large volume, which makes analysis impossible in regions with a high dose gradient; *(ii)* may be larger than the treated tumor volume. In certain treatment situations this characteristic may limit the definition of the spatial resolution of the dose; *(iii)* detectors are not equivalent to human tissues and *(iv) in* certain types of treatment there is the possibility of disturbing radiation fields, causing less accuracy in reading the exposure rate [5].

Alternative form of dosimetry employed to minimize field disturbance and uncertainties associated with dose recording is use of chemical dosimeters, especially polymer gel dosimeters. First polymer dosimeter developed and studied was *PAG* gel (polyacrylamide agarose gel), developed by Maryanski and collaborators [6]. This dosimetric solution is based on induced

copolymerization of acrylamide and N,N'-methylene-bis-acrylamide by ionizing radiation, where copolymers are homogeneously dissolved in an aqueous medium containing gelatin or agarose. This homogeneous solution is a means of interaction for radiation, because when photons are absorbed, attenuated or scattered by the dosimetric compound, (*i*) can interact directly with molecules of the monomers, resulting in ionizations and (*ii*) the production of free radicals, mainly by the radiolysis of the water molecules. However, the process *(i)* occurs on smaller scale, and the process *(ii)* is predominant due to the greater presence of solvent (water). Thus, radicals from radiolysis induce polymerization and the formation of crosslinks between monomers. The degree of polymerization and crosslinking formed in the irradiated medium is proportional to the absorbed dose. Use of agarose or gelatin would be a means of mechanical support, allowing the cross-links formed between the monomers to remain in the irradiated site, preserving and recording information about the spatial distribution of the dose. Subsequently, images generated on magnetic resonance imaging (MRI) or computed tomography (CT) are used to detect three-dimensionally changes generated by X radiation through polymerization caused in the dosimeter gel [7,8].

However, for better understanding of mechanisms of polymerization, a better understanding of the phenomena associated with the processes that trigger it and that allow the polymer chains formed to be proportional to the dose absorbed by the medium [2,6,9].

2. **BIBLIOGRAPHIC REVIEW**

2.1. Water radiolysis

As constitution of the *PAG* dosimeter gel is around 90% water, radiation will have a higher probability of interaction with water molecules. When these molecules interact with X-rays, they undergo dissociation, becoming other molecular products. This physical-chemical phenomenon is known as water radiolysis [9].

When a water molecule (H_2O) is irradiated, it undergoes ionization process and dissociates into two ions (ion pair), according to equation (1)

$$H_2O + h\nu \rightarrow HOH^+ + e^- \tag{1}$$

Following this initial reaction, several sequential reactions may occur. First, ion pair should rearrange itself, again generating a stable water molecule [9]. Second, if this rearrangement does not occur, possibly negative ion (electron) will attack another stable water molecule and consequently, a third type of reaction will occur according to equation (2)

$$H_2O + e^- \rightarrow HOH^- \tag{2}$$

HOH^+ and HOH^- ions are relatively instable and can dissociate into smaller molecules according to equations (3) and (4)

$$HOH^+ \rightarrow H^+ + OH^* \tag{3}$$

$$HOH^- \rightarrow OH^- + H^* \tag{4}$$

The result of water radiolysis is thus the formation of a pair of H^+ and OH^- ions and two free radicals H^* and OH^*. Ions H^+ and OH^- can again recombine [9].

H^* and OH* free radicals are neutral molecules containing a simple electronic parity in valence layer or at other external levels, thus becoming highly reactive. Free radicals are useless and exist with a lifetime of less than 1ms. During this time of existence, they can spread through the environment and interact in regions far from where they originated. Free radicals contain an excess of energy and in this way they can transfer this energy to other molecules, breaking their bonds and producing new ionization events [9].

H^* and OH^* ions are not free radicals produced only through the interaction of radiation with water. The free radical OH^* can join with another similar molecule and form hydrogen peroxide, according to equation (5)

$$OH^* + OH^* \rightarrow H_2O_2 \tag{5}$$

Hydrogen peroxide is highly harmful to the human body, being a toxic agent [9].

Free radical *H** can interact with molecular oxygen if it is present and then form the hydroperoxyl radical, according to equation (6)

$$H^* + O_2 \rightarrow HO_2^* \tag{6}$$

The hydroperoxyl radical, together with hydrogen peroxide are considered the most harmful agents of the water radiolysis process [9]. Hydrogen peroxide can also be generated by the reaction of two hydroperoxyl radicals, according to equation (7)

$$HO_2^* + HO_2^* \rightarrow H_2O_2 + O_2 \tag{7}$$

Many organic molecules, represented by *RH* can become reactive free radicals according to equation (8)

$$RH + h\nu \rightarrow RH^* \rightarrow H^* + R^* \tag{8}$$

When oxygen is present, other free radical species are possible, according to equation (9) [9]

$$R^* + O_2 \rightarrow RO_2^* \tag{9}$$

2.2. Free radical production

Despite the wide application of acrylic-derived monomers (such as acrylamide and N,N'-methylene-bis-acrylamide), little is known about the mechanisms of reaction and interaction with water radiolysis products [10].

Often, liquid organic substances are used as a solvent for monomers. In this case, during irradiation process, the generation of cation radicals or anions of liquid solution occurs, which also transform the molecules of monomers into free radicals, where they are also responsible for the

beginning of the polymerization process [11]. Thus, under certain conditions, intermediate reactions of water radiolysis induce polymerization process [12].

Polymer gel dosimeter is a hydrogel (water-based) gelatin in which monomers acrylamide and N,N'-methylene-bis-acrylamide are dissolved. When gel is irradiated, water molecules dissociate mainly into hydroxyl free radicals (OH^*) and hydrated electrons (e^-_{aq}), where carbon double bond of the N-N'-methylene-bis-acrylamide comonomer is broken, transforming it into an ion, according to equations (10) and (11)

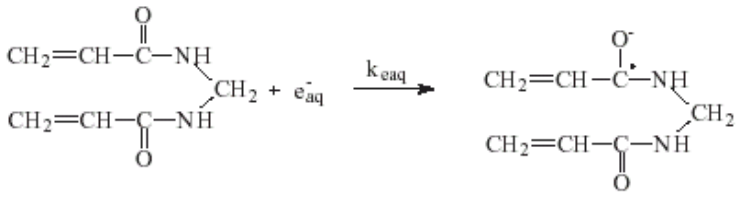

(10)

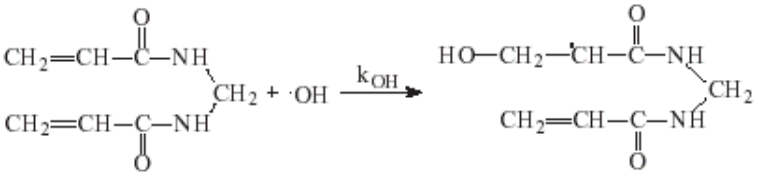

(11)

In equation (10) the formation of a radical anion in the carbonyl group of the molecule occurs through the interaction of the aqueous electron (e^-_{aq}) with this group [10].

Equation (11) is most likely form of hydroxyl (OH^*) attack on N,N'-methylene-bis-acrylamide molecule, interacting in the double bond of the vinyl group of the molecule [10].

Equation (12) demonstrates when H^* atom attacks the N,N'-methylene-bis-acrylamide molecule in the double bond of the carbonyl group, generating ion [10].

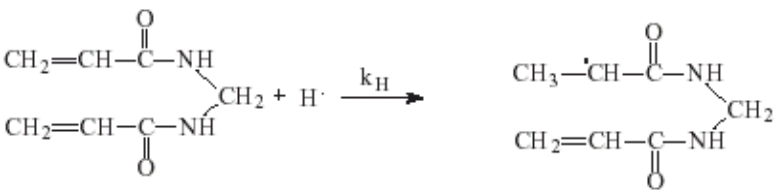

(12)

One way to regain a molecular equilibrium (lower energy ground state) is through protonation, as demonstrated in equation (13) [10]

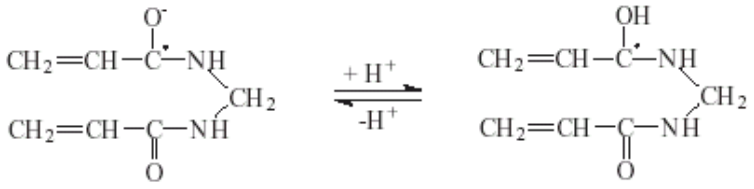

(13)

Equation (14) demonstrates that when the aqueous electron (e^-_{aq}) attacks acrylamide molecule, this attack occurs on the double bond of the carbonyl group of the molecule [10,11]

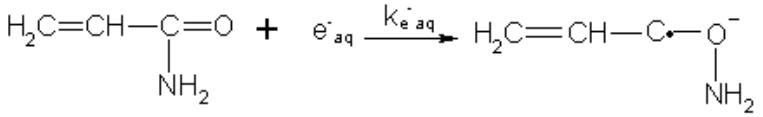

(14)

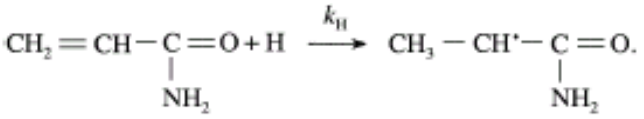

(15)

Equation (16) the interaction of the hydroxyl radical with the double bond of the vinyl group of the acrylamide molecule is represented [11].

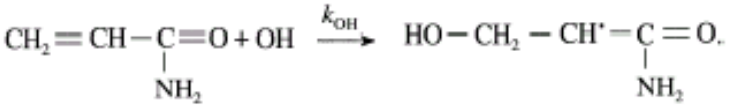

(16)

These initiation reactions are followed by propagation reactions, in which monomer radicals, demonstrated in equations (10), (11), (12), (14), (15), and (16) react with other monomers to form polymeric radical chains, as shown in Figure 1 [12].

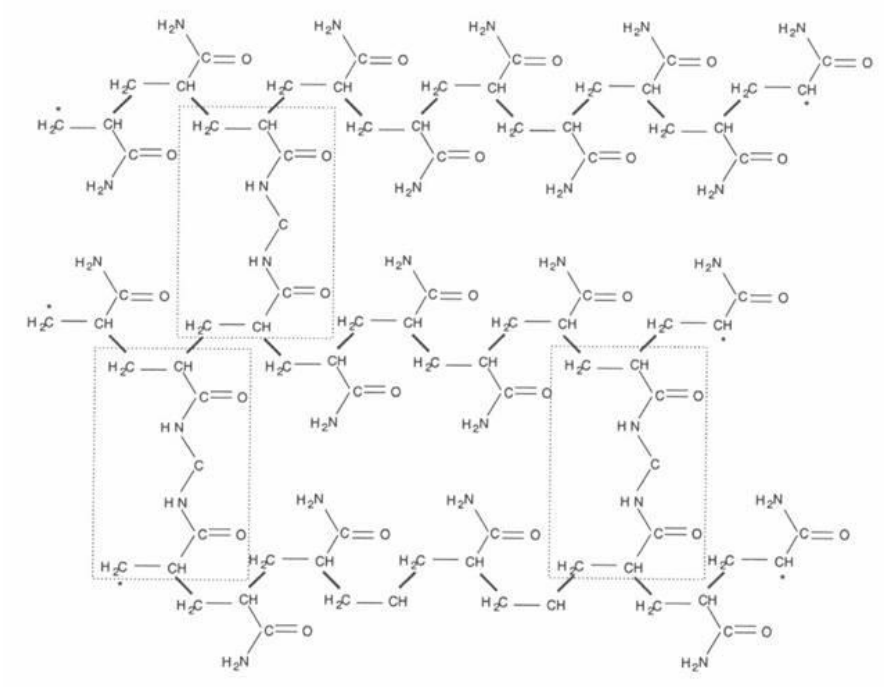

Figure *1: Formation of cross-linking agents (dotted) and polymer chains.*
Source: (HAMANN, 2009).

2.3. TRS 398

In 2000, the protocol for evaluating the quality of ionizing radiation beams in field of radiotherapy was launched: TRS 398 – "Determination of Absorbed Dose in Radiotherapy in External Beams – An International Code of Practice for Dosimetry Based on Absorbed Dose Patterns in Water". This protocol, which in addition to containing dosimetry recommendations for radiation beams in different energy ranges, introduced a very important conceptual change: instead of the absorbed dose being measured in air as it previously performed, it is now determined in the water through fantoma. In this way, the absorbed dose in the water, the *piori*, resembles the absorbed dose by human body. Thus, TRS 398 enabled (*i*) a more accurate dosimetry and (*ii*) reduced uncertainties associated with the dose determination process [1].

Therefore, for an initially more accurate verification of the dosimeter gel response behavior, its irradiation was based on the procedure presented in TRS 398. Factors such as source-detector distance (*SDD*), field size and depth of the detector in water were considered. Subsequently,

through magnetic resonance imaging, a response curve with an adjustment curve were determined to observe the behavior of the dosimeter gel.

3. MATERIALS AND METHODS

3.1. Irradiation ionization chamber

For irradiation the protocol presented in TRS 398 was followed [1]. Thus, the detector was submerged in water at a depth of 100 mm in relation to the surface (Figure 1) and at the isocenter point of the linear accelerator (source-detector distance of 1000 mm), with an irradiation field of 100x100 mm. After assembling set, it was waiting for the whole set to enter into thermal equilibrium to then occur the irradiation process. A total of five ionization chamber readings were performed (Table 1).

Table 1 – Reading of the ionization chamber for five exposures to the X-ray beam with energy of 6 MeV.

Exposure	**Reading value in ionization chamber (*nC*)**
1	95,78
2	95,77
3	95,78
4	95,77
5	95,78

Entire experimental arrangement was irradiated in a linear medical accelerator (LINAC) VARIAN 2100 (Oncoville – PR). Beam energy for X-rays was 6 MandV with absorbed dose in the middle of 5 Gy.

3.2. Preparation and irradiation of dosimeter gel

Dosimeter gel *nPAG* (normoxic polyacrylamide gel) with new chemical formulation was prepared [13]. In all, 14 vials were filled, each with a mass of 30 grams.

After preparing dosimetric material, the next step consisted of irradiation (LINAC VARIAN 2100 – Figure 2). In the methodology employed, the substitution method was adopted, that is, ionization chamber was replaced by the dosimetric samples. Therefore, specimens were irradiated following the TRS 398. The values used for doses were: 5, 10, 15, 20, 25 and 30 Gy. Two vials were not irradiated, which became standard samples.

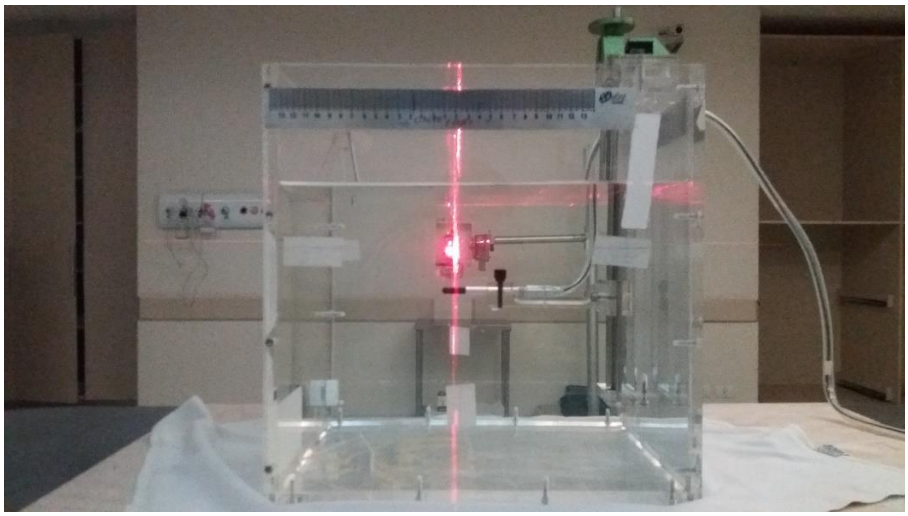

Figure 1: *Experimental arrangement for irradiation from the ionization chamber. Sensitive area (black region in the image) of the ionization chamber was at isocenter point of the equipment 100 mm deep from the surface. The irradiation field used was 100x100 mm.*

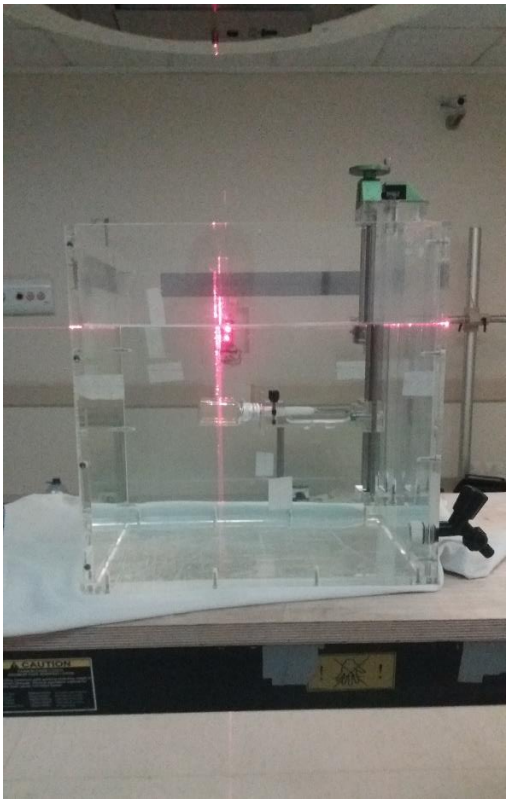

Figure 2: D*osimeter gel samples irradiated* by *replacement method, i.e., ionization chamber was replaced by the vials with dosimetric material. Depth, beam energy and irradiation field size were maintained. In the image, the center of the vial is observed at Linac isocenter point.*

3.3. Magnetic resonance imaging (MRI)

After irradiation of the dosimeter gel samples with different dose values, vials were submitted to magnetic resonance imaging (MRI) for the imaging process (Figure 3). GE SIGNA tomography (*General Electric* – Hospital das Clínicas-PR) with magnetic field of 1.5 Tesla for clinical use was employed to obtain images. Main parameters used for acquisition images are presented in Table 2.

Figure 3: *MRI equipment. Irradiated samples of the dosimeter gel were inserted into a head coil to obtain images.*

Table 2 – Parameters in MR for the acquisition of images with T2 weighting.

Scan sequence:	Echo Spin
Slice thickness:	5 mm
TR:	3,500 ms
TE:	240 ms
Coil:	head
Matrix size:	512x512
Nex (number of excites):	3

3.4. Curve response generation

Images generated in MRI were processed in the mathematical program JiveX. Thus, *ROI* (region of interest) analysis was performed in areas corresponding to the region irradiated vials. Thereby, slices and images generated from the 14 samples were analyzed. Statistical data such as (*i*) mean value, (*ii*) standard deviation, (*iii*) values of maximum and minimum and (*iv*) median were determined.

4. RESULTS AND DISCUSSIONS

Employing correction factors for ionization chamber reading as determined by TRS 398, values presented in Section 3.1 have been corrected. Physical quantity such as temperature, pressure, humidity and ionization chamber calibration correction factors, for example, were considered [1]. Thus, first (*i*) correction was made for the dosimetric readings carried by ionization chamber and (*ii*) real value of the absorbed dose in water depth where ionization chamber and dosimetric samples were irradiated were also determined.

Applying concept of extrapolation to obtained and corrected data, absorbed dose values were determined by dosimeter gel samples in the interval for which they were irradiated. These values are shown in Table 3.

Table 3 – Calculated dose for ionization chamber exposures

Expected Dose (Gy)	Corrected Dose (Gy)	Deviation (%)
5	5,08	0,01
10	10,16	0,01
15	15,24	0,01
20	20,32	0,01
25	25,4	0,01
30	30,48	0,01

Observed that deviation between the expected dose and corrected dose values was 1%. This deviation is within expected according to TECDOC 1151, which stipulates a maximum deviation of up to 2% [14].

Figure 4 corresponds to 30 g vials filled with dosimeter gel irradiated with different doses.

Previously developed studies employed polymer gel dosimetry only to analyze three dimensional dose distribution; this studies (*i*) not considering dosimeter gel response behavior as a function of dose deposition in the samples and (*ii*) without the using a protocol for sample irradiation [15,16]. Therefore, for a more accurate verification of behavior of dosimeter gel response, its irradiation was based on the protocol presented in TRS 398 [1].

The use of TRS 398 for irradiation of samples was: (*i*) for the traceability of dose in samples as function ionization chamber. Currently in radiotherapy centers, ionization chambers are primary standards for determining quality of the radiation beam. These centres have traceability of their ionization chambers in relation to a national primary laboratory. Thus, once calibrated and certified calibration, corrections for better dose estimate can be applied [1]; (*ii*) irradiation of samples at certain depth in relation to surface of input field (in this case this distance corresponds to 100 mm, as established in TRS 398) occurs to avoid contamination of photon beam by electrons. These electrons are result of the interaction of the X-beam with the collimator structure of linear accelerator. Finally (*iii*), with irradiation of samples following TRS 398 we have a more homogeneous dose deposition in samples. This occurs because the density of dosimetric solution is close to water density [17,18].

Figure 4: *Samples of 30* g *dosimeter gel irradiated with different dose values. From left to right in the image: 0, 5, 10, 15, 20, 25 and 30 Gy.*

Figure 5 shows an axial section of vials. This slice was obtained in MRI with T2 weighting. Image was generated with the parameters presented in Table 2, Section 3.3.

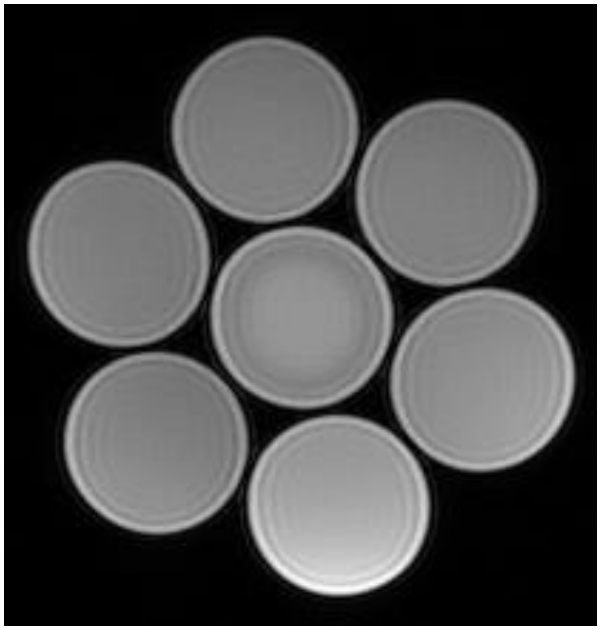

Figure 5: *Cross section samples filled with polymer gel after X-ray beam irradiation produced by LINAC. Slice were obtained with parameters presented in Table 2.*

Figure 6 demonstrates post processing of a (axial) section of images obtained by MRI. The resulting statistical analysis for each *ROI* in the image was generated using *JiveX*. Thus, through the mathematical program, slices and images associated with the 14 samples were analyzed.

ROI for statistical survey did not correspond to the entire area of dosimetric samples visualized in MRI slices. This fact occurred because near region of edges of each bottle there is a greater generation of noise. This signal fluctuation occurs due to differences in behavior before magnetic field between materials that make up the wall of the vials and dosimetric solution [19,20,21]. Thus, to minimize effects of this unwanted process, analysis was restricted to a more central area of each sample.

Table 4 corresponds (*i*) association between mean optical density value in analyzed region of *ROI*, (*ii*) absorbed dose value in each dosimeter gel sample and (*iii*) standard deviation associated with each *ROI* evaluated.

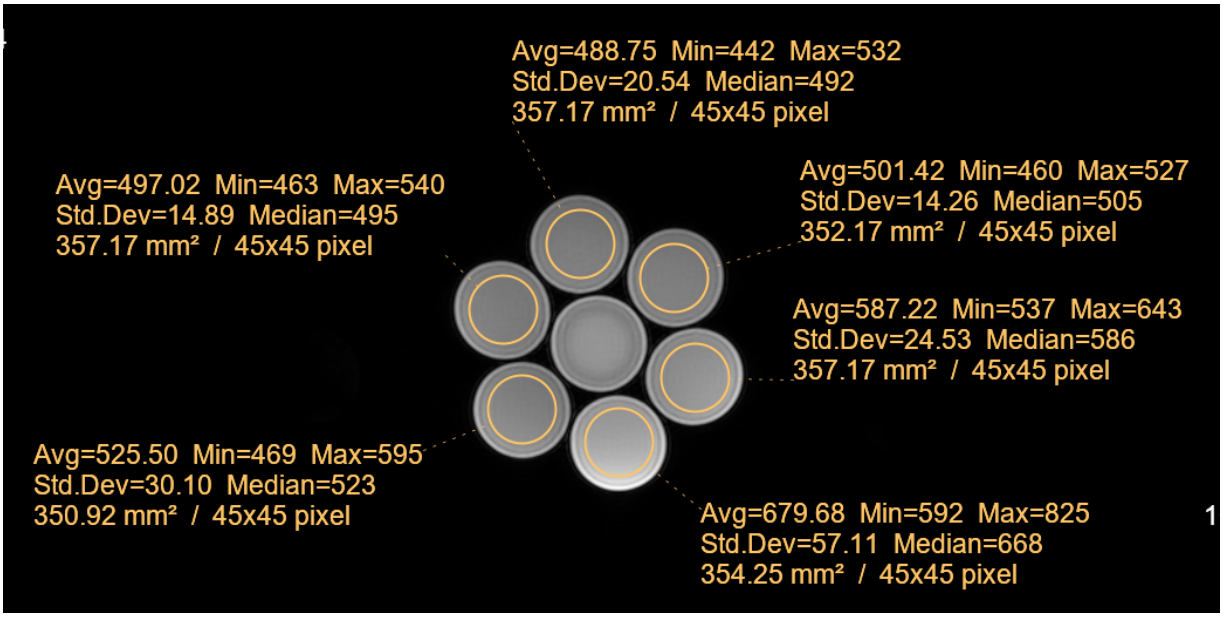

Figure 6: *Analysis of ROI regions (yellow circles in image) to determine the mean value of gray tone in each sample. Note that the mean value (Avg) of optical density in the analyzed ROI decreases with the increase of the dose value.*

Table 4 – Optical density values as a function of absorbed dose in each sample filled with dosimeter gel.

Optical Density (average value)	Standard Deviation	Absorbed Dose (Gy)
680	57	5
587	24	10
525	30	15
501	14	20
497	14	25
488	20	30

Figure 7 demonstrates response curve (points) generated by data presented in Table 4. These values were practically repeated in mathematical analysis used, slice by slice of the images obtained from the dosimetric material. Thus, the graph was determined by optical density (signal) as function

of absorbed dose in each sample. For the survey of the adjustment curve (in red), the regression method based on an exponential equation was employed [6,21,22,23].

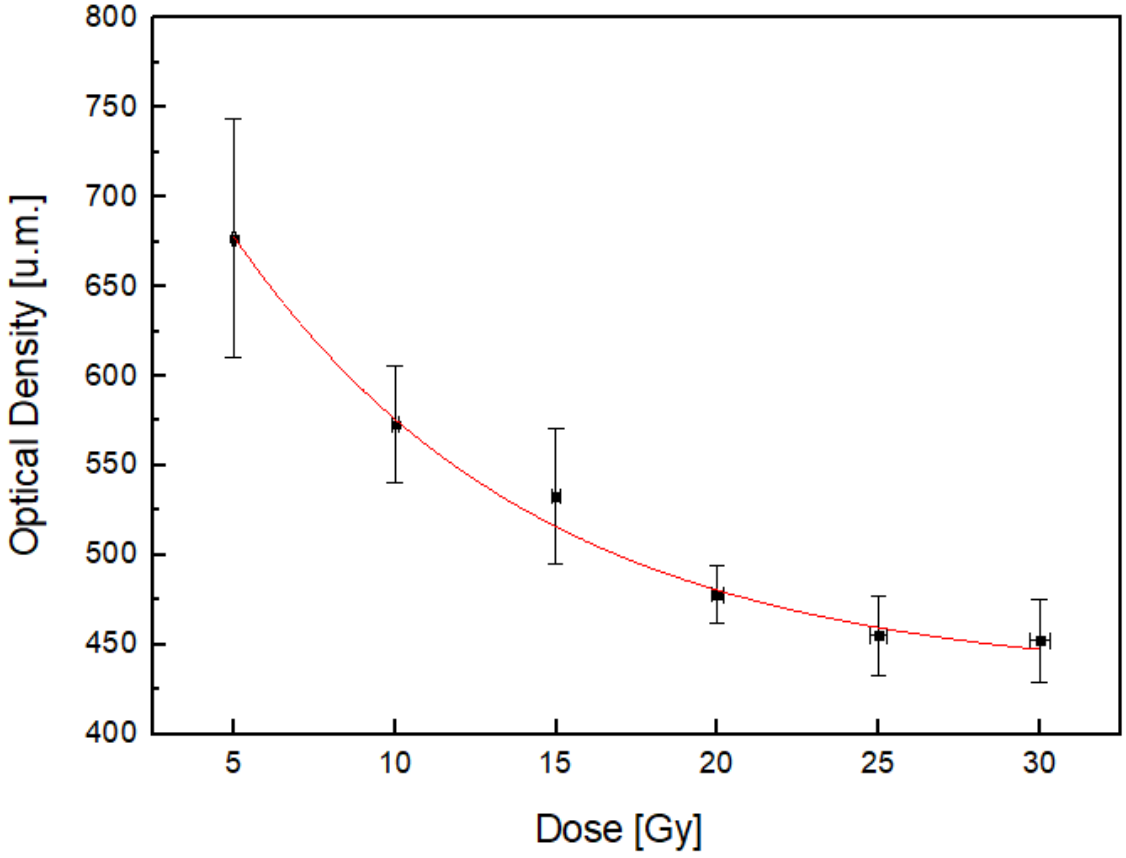

Figure 7: *Response curve (dark spots) and exponential regression process (red curve).*

Observing the adjustment curve in Figure 7 noticed that the value R^2 (*i*) is very close to unit (R^2 ~ 0.99); (*ii*) normalization curve is within the uncertainty values associated with each point of the response curve. Thus, R^2 presents satisfactory value [2,4]. Finally, (*iii*) greatest standard deviation presented at bottom of the curve is due to the sensitivity limit of the dosimeter gel [24,25]. More detailed studies will be developed in the future to better understanding of the associated mechanisms.

5. **CONCLUSIONS**

Due to high fraction of BIS crosslinking agents relative to the acrylamide fraction, the final polymer structure is not linear, but a three-dimensional polymeric network formed during irradiation process. It is believed that polymeric network generated consists of small spherical aggregates. Degree of polymerization is directly proportional function of the applied dose [6,15,16].

Therefore, polymeric aggregates cannot easily diffuse through gelatinous matrix. Chemical propagation reaction occurs only at irradiation site, at the site where chemical polymerization process started [6,16].

It should be noted that measurements performed with ionization chamber are absorbed dose at a certain point in space. Thus, calculations developed for dose determination are for the ionization chamber [1]. Dose measurement in dosimeter gel is a relative measure, within an area, obtained through the calibration curve. It does not replace chamber dosimetry measurements, being complementary or used for another purpose, such as three dimensional distribution of dose in volume [2,5,7].

Also observed that polymer gel dosimetry even presenting a new chemical formulation in its composition remains a promising tool. When associated with phantom can ensure quality and confidence during the planning, treatment and absorbed dose process in target volume. Dosimetric compound presents (*i*) equivalence to human tissue, (*ii*) three dimensional recording of isodose curves and (*iii*) greater temporal and dimensional stability in dose record (when compared to gel dosimetry Fricke, for example) [2,5,6,16].

ACKNOWLEDGMENT

We thank the financial support of CNPQ and CAPES agencies.

We also thank Physicist Otávio Riani de Oliveira of Oncoville Clinic (PR) where samples were irradiated in clinical LINAC; coordination of the UDIM of *Hospital de Clínicas* (CHC-PR), Physicist Renato Doro and radiology technologist Azir Pires and the technician Alessandro Frigel in aid to obtain MRI images.

REFERENCES

[1] TRS 398: **Absorbed Dose Determination in External Beam Radiotheraphy.** Available in: http://www-naweb.iaea.org/nahu/DMRP/documents/CoP_V12_2006-06-05.pdf>. Accessed May 2020

[2] MEEKS, S. L., BOVA, F. J., MARYANSKY, M. J., KENDRICK, L. A., KANADE, M. K., BUATTI, J.M., FRIEDMAN, W. A. "Image registration of BANG gel dose maps for quantitative dosimetry verification," **Int. J. Radiat. Oncol. Biol. Phys.,** vol. 43, no. 5, pp. 1135–1141, 1999.

[3] SCHLEGEL, W., BORTFELD, T., GROSU, A. L. **News technologies in Radiation Oncology,** 1st ed. Ger. 2006.

[4] BARAS, P., SEIMENIS, I., PAPAGIANNIS, P., PAPPAS, E., KIPOUROS, P. "Polymer gel dosimetry using a three-dimensional MRI acquisition technique.," **Med. Phys,** vol. 29, pp. 2506–2516, 2002.

[5] GAMBARINI, G., BRUSA, D., CARRARA, M., CASTELLANO, G., MARIANI, M., TOMATIS, M., VALENTE, M., VANOSSI, E. "Dose imaging in radiotherapy photon fields with Fricke and normoxic polymer Gels," **J. Phys. Conf. Ser.,** vol. 41, pp. 466–474, 2006.

[6] MARYANSKI, M. J.; GORE, J.C.; SCHULZ, R. J. "Relaxation enhancement in gels polymerized and cross-linked by ionizing irradiation: a new approach to 3D dosimetry by MRI.," **Magn. Mr. Reson. Imaging**, vol. 11, pp. 253–258, 1993.

[7] FUXMAN, A.M.; McAULEY, K.B.; SCHREINER, L. J. Modelling of polyacrylamide gel dosimeters with spatially non-uniform radiation dose distributions. **Chemical Engineering Science,** v. 60, p. 1277-1293, 2005.

[8] HILTS, M.; JIRASEK, A.; DUZENLI, C. Technical considerations for implementation of x-ray CT polymer gel dosimetry. **Phys. Med. Biol.,** v. 50, p. 1727-1745, 2005.

[9] BUSHONG, S.C. **Radiologic Science for Technologists.** 5th ed. Houston: Mosby Publishing House, 1993. 713 p.

[10] KOZICKI, M.; FILIPCZAK, K.; ROSIAK, J.M. Reactions of hydroxyl radicals, H atoms and hydrated electrons with N,N'-methylenebisacrylamide in aqueous solution. A pulse radiolysis study. **Radiation Physics and Chemistry,** v. 68, p. 827-835, 2003.

[11] KOZICKI, M.; KUJAWA, P.; ROSIAK, J.M. Pulse radiolysis study of diacrylate macromonomer in aqueous solution. **Radiation Physics and Chemistry,** v. 65, p. 133-139, 2002.

[12] WOJNÁROVITS, L.; TAKÁCS, E.; DAJKA, K.; D'ANGELANTONIO, M.; EMMI, S. S. Pulse radiolysis of acrylamide derivatives in dilute aqueous solution. **Radiation Physics and Chemistry,** v. 60, p. 337-343, 2001.

[13] HAMANN, J. H. **Polymer gel for dosimetry and quality control in equipment and sources eitters of ionizing radiation.** Depositor: João Henrique Hamann. BR102020013494-9. Deposit: June 2020.

[14] TECDOC 1151: **Physical Aspects of Quality Assurance in Radiotherapy.** 1st ed. Rio de Janeiro: INCA, 2000. 162 p.

[15] HAMANN, J. H. **Gel dosimeter type BANG-1: application in treatment planning by radiotherapy and qualitative evaluation through images obtained on magnetic resonance imaging.** 2009. Master's Thesis - Federal Technological University of Paraná, Curitiba.

[16] CRUZ, A. Development **of a dosimeter for three-dimensional analysis of ionizing radiation using polymer gel.** 2003. Master's Thesis - Federal Center of Technological Education of the State of Paraná, Curitiba.

[17] CUNNINGHAM, R. John; JOHNS, Harold E. **The Physics of Radiology.** 4th ed. Springfield: Charles C. Thomas Publisher. 796 p.

[18] KHAN, Faiz M. **The Physics of Radiation Therapy.** 2nd ed. Baltimore: Williams & Wilkins, 1994. 542 p.

[19] DEENE, Y.; WAGTER, C.; VAN DUYSE, B.; DERYCKE, S.; SNOW, W.; ACHTEN, E. Three-dimensional dosimetry using polymer gel and magnetic resonance imaging applied to the verification of conformal radiation therapy in head-and-neck cancer. **Radiotherapy and Oncology,** v. 48, p. 283-291, 1998.

[20] BLOEMBERGEN, N.; PURCELL, E.M.; POUND, R. V. Relaxation effects in nuclear magnetic resonance absorption. **Phys. Rev.,** v. 73, p. 679-712, 1948.

[21] DEENE, Y.; WALLE, R. de Van; ACHTEN, E.; WAGTER, C. Mathematical analysis and experimental investigation of noise in quantitative magnetic resonance imaging applied in polymer gel dosimetry. **Signal Processing,** v. 70, p. 85-101, 1998.

[22] SCHREINER, L. J. "True 3D chemical dosimetry (gel, plastics): Development and clinical role," **J. Phys.: Conf. To be.** 573, 2015.

[23] ZEHTABIAN, M., FAGHIHI, R., ZAHMATKESH, M. H., MEIGOONI, A. S., MOSLEH-SHIRAZI, M. A., MEHDIZADEH, S., SINA, S., BAGHERI, S. "Investigation of the dose rate dependency of the PAGAT gel dosimeter at low dose rates," **Radiation Measurements,** vol. 47, pp. 139–144, 2012.

[24] ISO/ASTM 52701 : **Guide for Performance Characterization of Dosimeters and Dosimetry Systems for Use in Radiation Processing.** 1st ed. Swizterland. ISO/ASTM. 2013. 11 p.

[25] ISO/ASTM 51261 ; **Standard Practice for Calibration of Routine Dosimetry Processing.** 2nd ed. Swizterland. 2013.ISO/ASTM. 2013. 20 p.